Solution to the Cosmic Ray Anisotropy Problem

Philipp Mertsch and Stefan Funk

Kavli Institute for Particle Astrophysics & Cosmology, 2575 Sand Hill Road, M/S 29, Menlo Park, California 94025, USA
(Received 19 August 2014; revised manuscript received 25 September 2014; published 13 January 2015)

In the standard diffusive picture for transport of cosmic rays (CRs), a gradient in the CR density induces a typically small, dipolar anisotropy in their arrival directions. This is being widely advertised as a tool for finding nearby sources. However, the predicted dipole amplitude at TeV and PeV energies exceeds the measured one by almost 2 orders of magnitude. Here, we critically examine the validity of this prediction, which is based on averaging over an ensemble of turbulent magnetic fields. We focus on (1) the deviations of the dipole in a particular random realization from the ensemble average, and (2) the possibility of a misalignment between the regular magnetic field and the CR gradient. We find that if the field direction and the gradient direction are close to ~90°, the dipole amplitude is considerably suppressed and can be reconciled with observations, which sheds light on a long-standing problem. Furthermore, we show that the dipole direction in general does not coincide with the gradient direction, thus hampering the search for nearby sources.

Cosmic rays (CRs) with energies between hundreds of MeV and at least a few PeV are commonly believed to be of Galactic origin. In the standard picture, the high degree of isotropy in their arrival directions is interpreted as evidence for diffusion that provides the necessary mechanism for efficiently randomizing their directions. On the other hand, in the case of a not perfectly symmetric distribution of sources with respect to the observer, a small degree of anisotropy, to first order a dipole in the arrival direction of cosmic rays, is to be expected. In particular, a (few) nearby source(s) can have a dominant effect on the distribution of arrival directions, which is why the observation of a dipole anisotropy has been advertised as a means of discovering these nearby sources [1–3]. Lately, this idea has gained currency in the context of finding the necessarily nearby (because of cooling losses) source(s) of high-energy electrons and positrons [4–6], which is (are) causing the rise in the positron fraction [7–9].

Given the high degree of isotropy, a perturbative approach is adopted in CR transport models, expanding the phase space density $f(\mathbf{r}, \mathbf{p}, t)$ into an isotropic part $f_0(\mathbf{r}, p, t)$ and a small correction $f_1(\mathbf{r}, \mathbf{p}, t)$. $f_1(\mathbf{r}, \mathbf{p}, t)$ is then related to the gradients of $f_0(\mathbf{r}, |\mathbf{p}|, t)$, the momentum gradient leading to the well-known Compton-Getting effect [10]; here, we focus on the spatial gradient. In a simple model of isotropic diffusion, the amplitude a of the dipole anisotropy, the relative difference between the fluxes in the maximum and minimum directions $\phi_{\max}$ and $\phi_{\min}$, computes as [11]

$$a = \frac{\phi_{\max} - \phi_{\min}}{\phi_{\max} + \phi_{\min}} = \frac{3D}{v} \frac{|\nabla f_0|}{f_0}, \qquad (1)$$

where D is the (local) spatial diffusion coefficient and $v \approx c$ is the CR speed. The dipole direction is opposite to that of

the CR gradient. For a given distribution of sources and extrapolating the diffusion coefficients measured through secondary-to-primary ratios like B/C at gigavolt to teravolt rigidities, one can first compute the CR density f_0 and through Eq. (1), the dipole amplitude. The rigidity dependence of the dipole amplitude results from both D and $|\nabla f_0|/f_0$.

Over the last decades, a large set of measurements of the dipole anisotropy has been accumulated at energies above a few TeV mostly from extensive air shower arrays [12–22]. The dipole amplitude decreases from ~10^{-3} at 10 TeV to
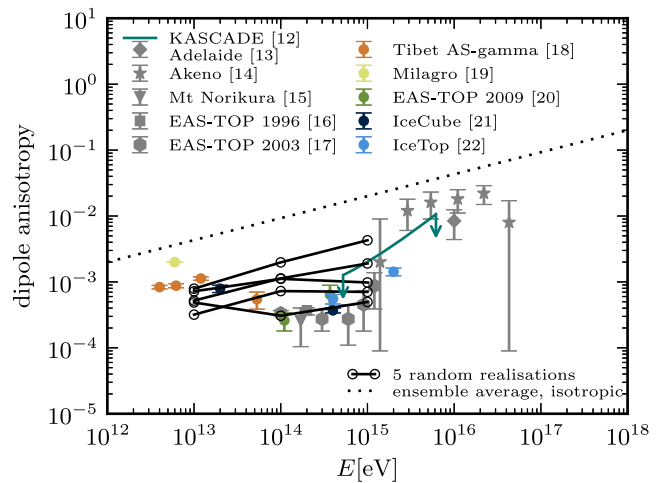

FIG. 1 (color online). The dipole anisotropy in the arrival directions of CRs, as predicted by an isotropic diffusion model [25] (dotted line) and measured by a variety of experiments [12–22]. The black filled circles, connected by solid lines, mark the dipole anisotropy predicted in five random realizations of the turbulent magnetic field and assuming a misalignment between the background magnetic field and CR gradient close to 90°.

$\sim 10^{-4}$ between 100 TeV and 1 PeV before it increases again. Here, we limit ourselves to energies below a few PeV where CRs are certainly of Galactic origin and where the composition is predominantly p and He. We show these measurements together with the prediction from a simple diffusion model in Fig. 1. It is evident (as has been known for a while [23,24]) that the diffusion model overpredicts the dipole amplitude by almost 2 orders of magnitude around 1 PeV.

This apparent discrepancy, dubbed the "CR anisotropy problem," has led to various modeling attempts. For example, it was pointed out that the point- and transientlike nature of CR sources, like supernova remnants, leads to fluctuations for different positions and periods of observations [24]; however, it has been shown by Monte Carlo methods [25–27] that even under favorable conditions an observation position or period in agreement with the measured dipole amplitude is unlikely. Furthermore, it has been suggested that the CR gradient would be smaller than usually predicted if the diffusion coefficient were allowed to spatially correlate with the sources of turbulence in the interstellar medium [28], e.g., supernova remnants, instead of being assumed to be constant. However, while this can alleviate some of the tension at hundreds of GeV, the predicted anisotropy at hundreds of TeV is still more than an order of magnitude too large.

It is instructive to revisit the derivation of Eq. (1) to investigate which assumptions need to be relaxed in order to reconcile the predicted dipole amplitude with measurements. For this, we adopt the framework of quasilinear theory [29] in which the magnetic field $\mathbf{B} = \mathbf{B}_0 + \delta\mathbf{B}$ is the sum of a regular field $\mathbf{B}_0$ and a turbulent field $\delta\mathbf{B}$ with $\delta B^2 = \int d^3k\, \delta\mathbf{B}^2(k) \ll |\mathbf{B}_0|^2$, and the turbulent field is evaluated along unperturbed trajectories. (The dipole anisotropy can also be computed in a more general framework (see, e.g., Ref. [30]), however, at the expense of not predicting the scattering rate from first principles.) Without loss of generality, we take $\mathbf{B}_0$ to point into the x direction, which is also defining the pitch angle $\mu = p_x/p$ of a particle of momentum $\mathbf{p} = (p_x, p_y, p_z)^T$. Under additional assumptions (e.g., after gyrophase averaging, see, e.g., Ref. [11] for details) the ensemble averaged distribution function can be expanded into an isotropic part and a pitch-angle dependent part: $\bar{f}(\mathbf{r}, \mathbf{p}, t) = f_0(\mathbf{r}, p, t) + f_1(\mathbf{r}, p, \mu, t)$. The first moment of the anisotropic part then determines the dipole amplitude (along the regular field)

$$a = \frac{\frac{3}{2}\int_{-1}^{1} d\mu\, \mu f_1(\mu)}{f_0} = \frac{3}{v}\frac{|\partial f_0/\partial x|}{f_0} D_{\parallel}. \qquad (2)$$

Here, $D_{\parallel} = D_{xx}$ is the parallel diffusion coefficient [31].

The derivation of Eq. (2) reveals two important limitations. First, the amplitude of the dipole anisotropy is an ensemble average, much like the underlying distribution function F is the average for the Gaussian random field $\delta\mathbf{B}$.

For propagation on Galactic scales, this is commonly justified by assuming ergodicity: for propagation times $t \gg L^2/D$, where $L \sim 100$ pc is the outer scale of turbulence in the interstellar medium (ISM), CRs from sources at kiloparsec distances will experience many different field configurations before observation. However, what is observed is not the time-averaged distribution function, but just a snapshot, which, as we will see, is affected by the (local) realization of $\delta\mathbf{B}$. (Also, note that typical observation times are shorter than the coherence time of the magnetic field turbulence.) The effect of the local field configuration was recently considered in the context of observed small scale anisotropies [30,32]. In particular, it was shown that the local $\delta\mathbf{B}$ is leading to nondiffusive behavior, dynamically generating and destroying correlations on all angular scales within a few scattering times τ_{sc} [30].

Second, Eq. (2) stresses the anisotropic nature of diffusion in the ISM and the possibility of misalignment between the CR gradient ∇f_0 and the regular field $\mathbf{B}_0$. For the case of a perfect misalignment of ∇f_0 and $\mathbf{B}_0$, the amplitude of the ensemble averaged dipole vanishes. In the absence of deviations from the ensemble average, this would already solve the CR anisotropy problem.

To investigate the interplay between these two effects, i.e., the deviation from the ensemble average in specific (local) realizations of $\delta\mathbf{B}$ on the one hand and the possible misalignment between ∇f_0 and $\mathbf{B}_0$ on the other hand, we employ a numerical simulation of the transport of charged particles through a turbulent magnetic field. Specifically, we backtrack particles; i.e., we follow particles of opposite charge backwards in time, injecting them in the opposite direction from which they would be observed. For observed directions $\mathbf{n_i} = \mathbf{p}_i\{0\}/p$ and positions $\mathbf{r}_i(0) = 0$ we obtain a set of backtracked trajectories, $\{(\mathbf{r}_i(t), \mathbf{p}_i(t))\}$. With these, and due to Liouville's theorem, we can compute the flux at $t = 0$, $\mathbf{r} = 0$ in the direction $\mathbf{n}_i$ from a given phase space density at an earlier time $-T < 0$, $f(\mathbf{r}_i(0), \mathbf{p}_i(0)) = f(\mathbf{r}_i(-T), \mathbf{p}_i(-T))$.

The relativistic equations of motion for charged particles are solved with a fifth order adaptive Runge-Kutta algorithm [33] and we consider particles with rigidities of 10, 100, and 1000 TV, neglecting the finite energy resolution of the experimental data. The level of turbulence $\eta \equiv \delta B^2/(\delta B^2 + B_0^2)$ is very uncertain, especially in the local ISM. On large scales, Faraday rotation measurements point to regular fields as low as $B_0 \simeq (1.4 \pm 0.2)\ \mu$G, which with a total field of 6 μG (from equipartition) gives $\eta \simeq 0.96$ [34]. On the other hand, to reproduce the grammage inferred from nuclear secondary-to-primary ratios, a much smaller $\eta \lesssim 0.02$ would be needed [35]. To bracket these vastly different estimates (and to ease comparison with other numerical studies [36,37]) we adopt two values: $\eta = 1$ and 0.1. The turbulent field is computed on a set of nested grids [36] with a Kolmogorov spectrum,

an outer scale $L = 100$ pc, and a total (rms) field strength of 4 μG. We have checked that averaging over many different realizations of $\delta\mathbf{B}$ we recover diffuse behavior. In particular, adopting the parameters of Refs. [36,37] we reproduce the inferred pitch-angle scattering times and diffusion coefficients.

We have confirmed that our computation reproduces the expected anisotropies at $t = 0$ for different combinations of (in)homogeneous and (an)isotropic distribution functions at $t = -T$. Trivially, a homogeneous and isotropic phase space density at $-T$ leads to no anisotropy. A homogeneous distribution of dipoles at $-T$ leads not only to a dipole but also to power for larger multipole moments ℓ, all of which are eventually decaying exponentially with a time constant $\tau_{\rm sc}/\ell(\ell + 1)$ [30]. The scenario we are most interested in here is an initial gradient in the phase space distribution: after a few $\tau_{\rm sc}$, the distribution of arrival directions converges, irrespective of the initial angular distribution. We observe anisotropies extending to the highest multipoles allowed by our angular resolution, which are eventually all powered by the spatial gradient in the initial distribution function.

Every spatial distribution at times $-T$ can be expanded into a spatially homogeneous part, a gradient, and higher derivatives. We assume that the higher derivatives are subdominant and adopt the (ensemble averaged) gradient from the diffusion model. We read off this gradient for the average source distribution from Fig. 2(a) of Ref. [25] adopting their parametrization of the diffusion coefficient measured from B/C.

We start by presenting our results for the case of isotropic turbulence without a regular field, i.e., $\eta = 1$. In Fig. 2, we show the dipole directions by the black circles, obtained for 50 random realizations of the magnetic field, a CR gradient in (long, lat) = $(90°, 0°)$, and 1 PV particles. There is considerable scatter in the dipole directions around the predicted value from the diffusion model (indicated by the green diamond). The mean dipole of the 50 random realizations (indicated by the red square), however, reproduces the predicted dipole very well. There is also scatter in the *amplitudes* of individual dipoles, and on average their amplitude is larger than that of the predicted dipole. This is also shown in Fig. 3, where we have varied the direction of the CR gradient: each vertical slice is a (normalized) histogram of the distribution of the dipole amplitudes. The red (green) line marks the average amplitude from the 50 random realizations (the predicted amplitude from the isotropic diffusion model) corresponding to the sizes of the red square (green diamond) in Fig. 2. As expected there is no preferred direction. At the same time, while there is some scatter around the predicted dipole amplitude, it is too little to explain the small experimental upper limit and measurement of a few times 10^{-4}.

The results for the case with a strong regular field differ significantly. Although ∇f_0 is still at (long, lat) = $(90°, 0°)$, the dipole directions now cluster
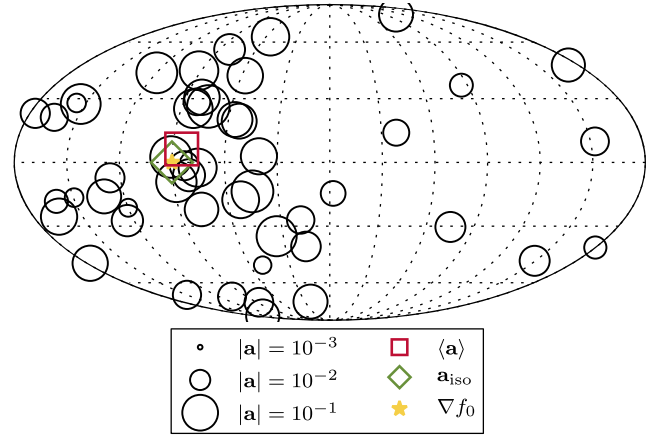

FIG. 2 (color online). Sky map of dipole directions in 50 random realizations of the local turbulent magnetic field ($\eta = 1$) at 1 PV. The center and radius of each black circle shows the dipole direction and amplitude in one random realization, respectively. The yellow star shows the direction of the assumed CR gradient, the green diamond the predicted value from an isotropic diffusion model, and the red square the average of the 50 magnetic field configurations.

around the $\mathbf{B}_0$ direction, which is at (long, lat) = $(0°, 0°)$, see Fig. 4. It is also apparent that for this misalignment the amplitudes are markedly suppressed. While this was already expected for the ensemble averaged dipole, see Eq. (2), there is considerable scatter, both in amplitude and in direction. We emphasize that this is due to the random nature of $\delta\mathbf{B}$, which is not accounted for in Eq. (2), and that the dipole is likely in the direction of the *total* $\mathbf{B}$ as sampled by the CR trajectories. In Fig. 5, we show the distribution of
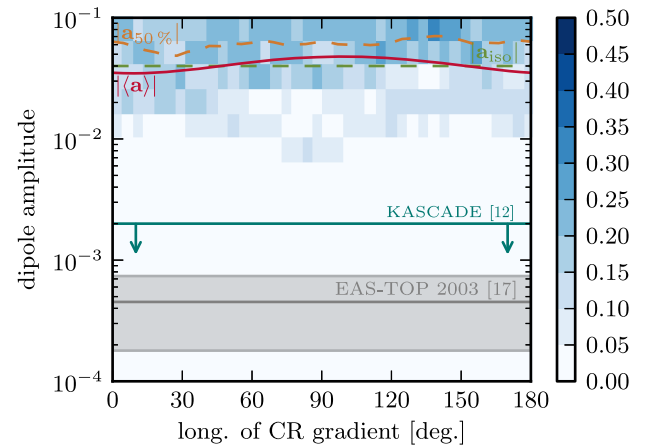

FIG. 3 (color online). The distribution of dipole amplitudes as a function of the longitude of the CR gradient at 1 PV for $\eta = 1$. Each vertical slice is the normalized histogram for a gradient direction. We also show the median (orange dashed line) and amplitude of the (vectorial) mean (red solid line), together with the prediction for isotropic diffusion (green dashed line). The cyan solid line and gray band show the KASCADE upper limit and the EAS-TOP measurement at ~1 PeV, respectively.
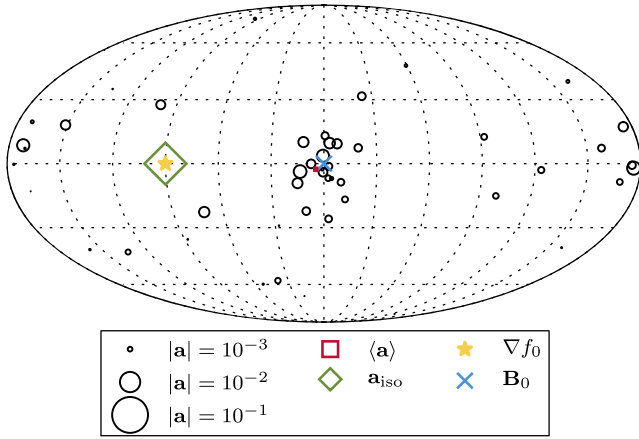
FIG. 4 (color online).   Same as Fig. 2, but for a small turbulent field on top of a regular field ($\eta = 0.1$), indicated by the blue cross.

dipole amplitudes as a function of longitude of ∇f_0 (here, that is the angle between ∇f_0 and $\mathbf{B}_0$). The distribution shows the expected cosine behavior and for most angles the scatter is small. For near-to-perfect misalignment, however, we find that the majority of random realizations have a dipole amplitude below the KASCADE upper limit and of order 20% are consistent with the EAS-TOP 2003 measurement.

In Fig. 1, we have shown the dipole amplitudes for five random field realizations at 10 TeV, 100 TeV, and 1 PeV (assuming protons) for an angle $\sim 90°$ between the CR gradient and regular field. We note that while for three random realizations the amplitudes increase with energy as expected, the other two show nontrivial energy dependences, one even closely tracing the experimentally observed decline and rise from 10 to 100 TeV and on to 1 PeV. This nonstandard energy dependence is evidence of particles of different rigidities sampling different parts of the local turbulent field.
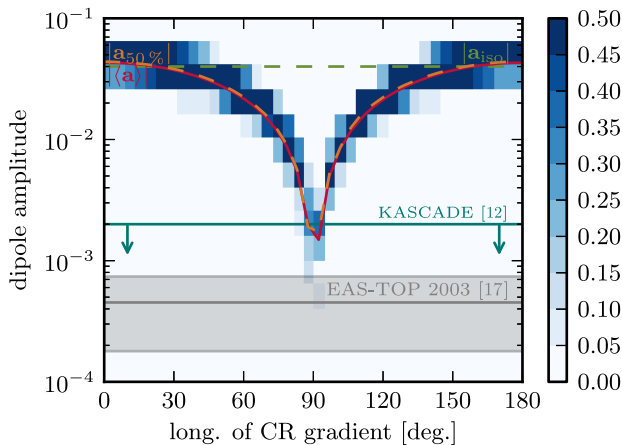

FIG. 5 (color online).   Same as Fig. 3, but for a small turbulent field on top of a regular field ($\eta = 0.1$).

One might wonder how a possible energy dependence of the gradient direction would affect our results. First, we note that to achieve the necessary suppression, the CR gradient and the regular magnetic field need to be perpendicular only to within $\sim 10°$ (see Fig. 5). Second, it has been shown in computations of the CR gradient that its direction is relatively stable; i.e., it varies by less than $10°$ for a relatively wide range of energies [25]. Therefore, even with finite energy resolution the suppression of the dipole can be maintained for energies between $\sim 10^{14}$ and 10^{15} eV, whereas outside this interval the misalignment could be less severe, thus causing less suppression of the dipole amplitude.

To a certain degree, the rigidity-dependent sampling of the magnetic field could also cause the rise in anisotropy above a few PeV, which seems to be observed in earlier measurements [13,14]. (We caution, however, that contemporary experiments, e.g., Ref. [12], have so far only placed upper limits.) After a few scattering times, particles of rigidity $\mathcal{R}_{\mathrm{Pev}}$PeV cover on average distances of a few times $\sqrt{4D_{\parallel}\tau_{\mathrm{sc}}} \simeq 100^{q-1}\mathrm{pc}(\delta B/B_0)^{-2}(\mathcal{R}_{\mathrm{PV}}/B_{0,\mu\mathrm{G}})^{2-q}$ (here, $q = 5/3$ is the Kolmogorov spectral index). With the parameters adopted above for the $\eta = 0.1$ case, this computes as a few hundred parsecs at 1 PV and more than doubles with every decade in rigidity. Therefore, at higher rigidities a larger part of the turbulent field is being sampled, with the large-scale modes ($1/k \ll r_L$) effectively contributing to the background field. This already leads to the nonstandard rigidity dependence for the energy range shown in Fig. 1, but as the amplitude of the turbulent modes grows with scale, this effect is expected to get stronger with rigidity. Furthermore, in numerically computing the trajectories of CRs, we have neglected the possibility of escape from the CR halo, which is only valid if the distances travelled are much smaller than the size of the CR halo. Beyond petavolt rigidities, this assumption breaks down, which will lead to a higher anisotropy amplitude. Finally, at even higher rigidities, the gyroradius approaches the scale of variations in $\mathbf{B}_0$, such that gradient and curvature drifts cannot be neglected anymore, leading to additional contributions to the anisotropy. We leave a detailed study of these effects to future work.

Our conclusions are twofold. First, it is not possible to determine the direction of the CR gradient (and thus the direction of the closest, dominant source or the bulk of sources) from the dipole direction: for strong turbulence, there is considerable scatter between the CR gradient and the dipole directions in random realizations; for weak turbulence, the dipole directions scatter around the regular field direction rather than around the CR gradient. Second, the small observed dipole amplitudes between ~ 100 TeV and 1 PeV can be understood in the presence of a strong regular field only if the CR gradient and the regular field are almost maximally misaligned. This opens up the possibility of determining the direction of the regular

magnetic field, if the CR gradient could be reliably predicted or determined by other means, e.g., diffuse gamma-ray backgrounds [38]. We conclude by noting that in a similar way that the dipole depends on the regular field direction, the higher multipoles of the arrival direction encode information about the higher moments of the (turbulent) local magnetic field. While it is computationally very challenging to solve the inverse problem of inferring the latter from the former, observations of CR arrival directions might soon prove one of the most valuable probes of the nearby Galactic magnetic field.

[1] V. S. Ptuskin and J. F. Ormes, in *Proceedings of the 24th International Cosmic Ray Conference, Rome, 1995*, edited by N. Iucci and E. Lamanna (International Union of Pure and Applied Physics, London, 1995) Vol. 3, 56.
[2] I. Buesching, O. C. de Jager, M. S. Potgieter, and C. Venter, Astrophys. J. **678**, L39 (2008).
[3] L. G. Sveshnikova, O. N. Strelnikova, and V. S. Ptuskin, Astropart. Phys. **50–52**, 33 (2013).
[4] G. Di Bernardo, C. Evoli, D. Gaggero, D. Grasso, L. Maccione, and M. N. Mazziotta *et al.*, Astropart. Phys. **34**, 528 (2011).
[5] E. Borriello, L. Maccione, and A. Cuoco, Astropart. Phys. **35**, 537 (2012).
[6] T. Linden and S. Profumo, Astrophys. J. **772**, 18 (2013).
[7] O. Adriani *et al.*, Nature (London) **458**, 607 (2009).
[8] M. Ackermann *et al.*, Phys. Rev. Lett. **108**, 011103 (2012).
[9] M. Aguilar *et al.*, Phys. Rev. Lett. **110**, 141102 (2013).
[10] A. H. Compton and I. A. Getting, Phys. Rev. **47**, 817 (1935).
[11] V. L. Ginzburg *et al.*, *Astrophysics of Cosmic Rays* (North-Holland, Amsterdam, 1990).
[12] T. Antoni *et al.*, Astrophys. J. **604**, 687 (2004).
[13] P. R. Gerhardy and R. W. Clay, J. Phys. G **9**, 1279 (1983).
[14] T. Kifune *et al.*, J. Phys. G **12**, 129 (1986).
[15] K. Nagashima *et al.*, in *Proceedings of the 21st International Cosmic Ray Conference, Adelaide, 1990*, edited by R. J. Protheroe Vol. (3, 180.
[16] M. Aglietta *et al.*, Astrophys. J. **470**, 501 (1996).
[17] M. Aglietta *et al.*, *Proceedings of the 28th International Cosmic Ray Conference, Tsukuba, 2003* Vol. 4, 183.
[18] M. Amenomori *et al.*, Astrophys. J. **626**, L29 (2005).
[19] A. A. Abdo *et al.*, Astrophys. J. **698**, 2121 (2009).
[20] M. Aglietta *et al.*, Astrophys. J. **692**, L130 (2009).
[21] R. Abbasi *et al.*, Astrophys. J. **746**, 33 (2012).
[22] M. G. Aartsen *et al.*, Astrophys. J. **765**, 55 (2013).
[23] A. M. Hillas, J. Phys. G **31**, R95 (2005).
[24] V. S. Ptuskin, F. C. Jones, E. S. Seo, and R. Sina, Adv. Space Res. **37**, 1909 (2006).
[25] P. Blasi and E. Amato, J. Cosmol. Astropart. Phys. 01 (2012) 011.
[26] M. Pohl and D. Eichler, Astrophys. J. **766**, 4 (2013).
[27] R. Kumar and D. Eichler, Astrophys. J. **785**, 129 (2014).
[28] C. Evoli, D. Gaggero, D. Grasso, and L. Maccione, Phys. Rev. Lett. **108**, 211102 (2012).
[29] J. R. Jokipii, Astrophys. J. **146**, 480 (1966).
[30] M. Ahlers, Phys. Rev. Lett. **112**, 021101 (2014).
[31] N. A. Schwadron, F. C. Adams, E. R. Christian, P. Desiati, P. Frisch, H. O. Funsten, J. R. Jokipii, D. J. McComas, E. Moebius, and G. P. Zank, Science **343**, 988 (2014).
[32] G. Giacinti and G. Sigl, Phys. Rev. Lett. **109**, 071101 (2012).
[33] M. S. Sutherland, B. M. Baughman, and J. J. Beatty, Astropart. Phys. **34**, 198 (2010).
[34] R. Beck and R. Wielebinski, in *Galactic Structure and Stellar Populations*, edited by G. Gilmore, Planets, Stars and Stellar Systems Vol. 5, (Springer, Berlin, 2013).
[35] D. De Marco, P. Blasi, and T. Stanev, J. Cosmol. Astropart. Phys. 06 (2007) 027.
[36] G. Giacinti, M. Kachelrieß, D. V Semikoz, and G. Sigl, J. Cosmol. Astropart. Phys. 07 (2012) 031.
[37] F. Casse, M. Lemoine, and G. Pelletier, Phys. Rev. D **65**, 023002 (2001).
[38] M. Ackermann *et al.*, Astrophys. J. **710**, 133 (2010).
[39] K. M. Gorski, E. Hivon, A. J. Banday, B. D. Wandelt, F. K. Hansen, M. Reinecke, and M. Bartelmann, Astrophys. J. **622**, 759 (2005), http://healpix.sourceforge.net.